

# Intermolecular and diffusive dynamics of pure acetonitrile isotopomers studied by depolarized Rayleigh scattering and femtosecond optical kerr effect

P. Foggi<sup>1,2,a</sup>, P. Bartolini<sup>1</sup>, M. Bellini<sup>3</sup>, M.G. Giorgini<sup>4</sup>, A. Morresi<sup>2</sup>, P. Sassi<sup>2</sup>, and R.S. Cataliotti<sup>2,5</sup>

<sup>1</sup> LENS, via Nello Carrara 1 and INFN Unitá di Firenze, via Giovanni Sansone 1, Polo Scientifico Universitario, Sesto F.no, 50019 Florence, Italy

<sup>2</sup> Dipartimento di Chimica, Università di Perugia, via Elce di Sotto 8, 06100 Perugia, Italy

<sup>3</sup> INOA, Largo E. Fermi 6, 50125 Firenze, Italy

<sup>4</sup> Dipartimento di Chimica Fisica ed Inorganica, Università di Bologna, viale Risorgimento 4, 40136 Bologna, Italy

<sup>5</sup> INFN, Unitá di Catania, Corso Italia 57, 95100 Catania, Italy

Received 21 July 2002

Published online 1st October 2002 – © EDP Sciences, Società Italiana di Fisica, Springer-Verlag 2002

**Abstract.** The relaxation dynamics of pure acetonitrile isotopomers has been investigated in the temperature range 8 to 75 °C. The overall response of the liquid is measured either recording directly the decay of the optical Kerr signal with heterodyne detection (OHD-OKE) and Fourier transforming the depolarized Rayleigh scattering spectra (DRS). The OHD-OKE signals show a decay that can be described by a bi-exponential law. At some temperatures, stressing to a maximum level the sensitivity of the OHD-OKE experimental set-up, a damped oscillation is observed on top of the fast decay component. The two techniques provide same results with a high level of reproducibility, as far as the slow component is concerned. This latter is described by an exponential law with the time constants ranging in the interval 2.0 to 0.85 ps in the light and approximately in the same interval in the deuterated molecule. The decays are, at all temperatures, well reproduced by the extended diffusion  $J$ -model. The fast component, better observed with the OHD-OKE experiments in a restricted temperature range, has time constants ranging from 550 to 350 fs. After the subtraction of the curve due to the slower decay component, the data have also been analyzed by Fourier transforming the fast part of the decay. The  $\chi''$  spectrum then consists of a broad (approximately 80 cm<sup>-1</sup> wide) band centered at 50 cm<sup>-1</sup>. This band is interpreted as the manifestation of intermolecular vibrational motions.

**PACS.** 61.20.Lc Time-dependent properties; relaxation – 33.20.Fb Raman and Rayleigh spectra (including optical scattering) – 78.47.+p Time-resolved optical spectroscopies and other ultrafast optical measurements in condensed matter

## 1 Introduction

The low frequency domain of the light scattering spectral density in the liquid state is a peculiar region where the discrimination among different relaxation processes such as molecular reorientations, collision induced scattering (CIS), dipole-induced dipole interactions (DID), and intermolecular motions as for instance pseudo-lattice phonons, is not so far very well defined. The principal reason for this lies on the fact that all the above mentioned processes cannot be identified separately by acting on classical experimental variables as temperature, pressure and molar fraction in the case of mixtures. In the recent past many papers have been published on the dy-

namics of simple liquids, with the aim of understanding the behavior of such molecular systems following rapid perturbations of the equilibrium variables and providing a more complete picture of the interactions occurring in solutions and of the solvent effect on simple intra- and intermolecular reactions [1–25]. Depolarized Rayleigh scattering (DRS) and time resolved optical Kerr effect (OKE) are proper experimental tools to investigate the fast response of simple molecular liquids. They have the same content of information being correlated by a Fourier transformation (FT) [6–35]. As proposed by Gordon in a series of fundamental articles [36–38], the power spectra can be represented by the FT of the time-correlation function. In particular DRS is proportional to the FT of the susceptibility fluctuations' correlation function of the

<sup>a</sup> e-mail: foggi@colonnello.lens.unifi.it

system. On the other side the OKE, depending on the third order susceptibility, contains contributions from the third order electronic response and from the first order nuclear susceptibility correlation function [39]. It has been recently demonstrated experimentally that they do have the same content of information [35]. We ourselves have confirmed this theoretical argument by a numerical comparison of the orientational relaxation times and orientational activation energy obtained in two experiments performed on nitromethane [15,20], concluding that they single out the same dynamical processes. Experimental limitations make the two techniques complementary rather than equivalent, being the DRS less sensitive in the wings (short times) and the OKE experiment less sensitive to the slower dynamics (long times). Both the techniques provide information on the collective dynamics occurring in the liquids.

A general observation is that in molecular liquids it is possible to distinguish two temporal regimes: a first one, on average below 1 ps, due to several contributions which govern the collective polarizability, and a second one longer, which is interpreted as due to diffusive motions [1–14,16,17,21]. Recently it has been observed that even below 1 ps, at least the symmetric-top molecular liquids show dynamics following an exponential decay law and that the decay constant scales with  $\eta/T$ , where  $\eta$  is the share viscosity of the medium [24].

Strictly speaking the description of the liquid state dynamics in terms of diffusive motions holds in the case of the interaction between a big solute molecule embedded in small molecules acting as solvent. Such is the assumption in the Debye-Stokes-Einstein (DSE) theory. The extension of the DSE model to pure liquids or solutions of molecules of comparable size, where a molecule interacts with other neighbors of the same type and/or dimensions, is not obvious. Nevertheless many experimental results have been interpreted in the light of the DSE model. This derives from the observation that often the dependence of decay times is related linearly to the ratio  $\eta/T$  [40].

Acetonitrile can be considered a prototype among the polar liquids since it is one of the most utilized solvents due to its strong dipole moment and the almost no-tendency to give very stable aggregates [6]. The average structure lifetime is shorter than the orientational correlation time at all temperatures [18]. Furthermore, under certain aspects, the spectroscopy of acetonitrile is quite easy to be understood, being the molecule a true symmetric top system. The dynamics of this solvent has been the object of several experimental and theoretical studies [6,12,14,22–34]. Even very recently Fourkas and his coworkers proposed in a couple of papers [22,24] a new analysis of the short time (<1 ps) regime of the OHD-OKE signal decay of pure acetonitrile.

In this article we report on the results obtained utilizing optically heterodyne detected OKE (OHD-OKE) experiments and, as far as the slower dynamics is concerned, DRS measurements on liquid acetonitrile and its deuterated analog in the temperature range 8 to 75 °C (281–348 K).

## 2 Experimental and data handling

### 2.1 Steady-state experiments

The experimental apparatus used to obtain the DRS spectral distributions of the pure compound and for monitoring the temperature has been described elsewhere [27]. A brief description will follow. DRS were obtained by focusing 0.2 W of the 514.5 nm radiation of an Ar<sup>+</sup> laser on the sample cell. The spectra were collected over an extended spectral range (300 cm<sup>-1</sup>) with an HV polarization configuration in a 90 degree scattering geometry. The signals were corrected for the Tyndall scattering peak and Fourier analysed in the time domain where we have applied the correction for the spectral slit distortion to get the orientational correlation functions. Measurements were also performed on diluted solutions (mole fraction  $x = 0.1$ ) of CH<sub>3</sub>CN in CCl<sub>4</sub> and in a mixture of isopentane ( $\eta = 0.223$  cp at 293 K) and CCl<sub>4</sub> ( $\eta = 0.969$  cp at 293 K). This mixture results isoviscous with acetonitrile ( $\eta = 0.359$  cp at 293 K). The measurements on the diluted solutions were carried out using a Spex 1404 spectrometer equipped with a liquid nitrogen cooled CCD detector and were sampled at 0.3 cm<sup>-1</sup> corresponding to one pixel of the CCD array; the collection was made over 260 cm<sup>-1</sup> corresponding to the CCD active area. Within the observed region ( $\pm 130$  cm<sup>-1</sup> around the maximum) the lower signal was of the order of 1000 counts/s where the peak was about 60000 counts/s (saturation is at 62000); the noise (dark counts) was 30 counts/s. The intensity of the Tyndall contribution, after filtering the liquid with Millipore filters, is less than 25% of the maximum intensity.

The orientational correlation functions have been analysed by bi-exponential decays in a fitting procedure that leads to the characteristic times. The slow decay time constants are reported in Table 1 whereas the correlation functions at two temperatures for the light and the deuterated molecule are shown in Figures 1a and 1b respectively.

To enlighten the spectral structure of the Rayleigh wings we have investigated the Rayleigh spectral distribution in a reduced form as [41]:

$$I \propto (\nu - \nu_0)^4 \left( n(\nu) + 1 \right) \chi^2(\nu) \quad (1)$$

where  $\nu_0$  is the exciting line frequency and  $n(\nu)$  the Bose factor. The results are shown in Figure 2.

### 2.2 The time-resolved OHD-OKE experiments

The experimental setup of the time resolved OHD-OKE apparatus, earlier described in reference [42], is shown in Figure 3. As previously mentioned, the signal has been measured with heterodyne detection and two different wavelengths are utilized for the pump and the probe pulses. Some details of the dual color OHD-OKE experiment relevant to the data treatment are reported in the Appendix.

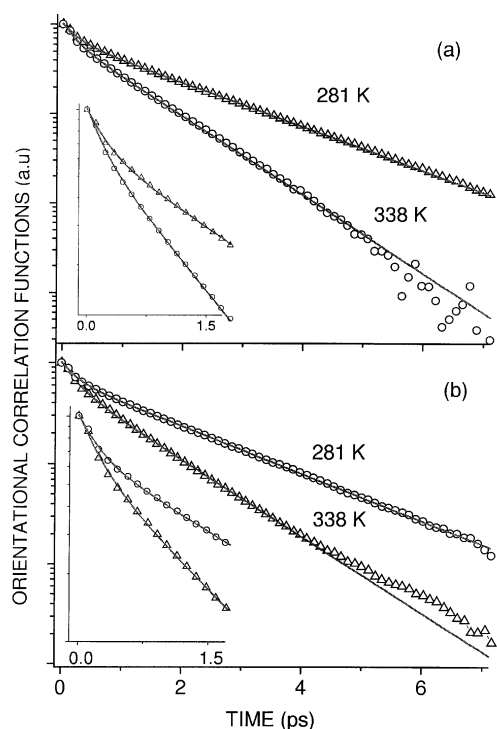


**Fig. 1.** Time correlation functions obtained from DRS spectra for (a)  $\text{CH}_3\text{CN}$  and (b)  $\text{CD}_3\text{CN}$  at 281 and 338 K. The insets report the short time region where the bi-exponential nature of the orientational decay can be observed.

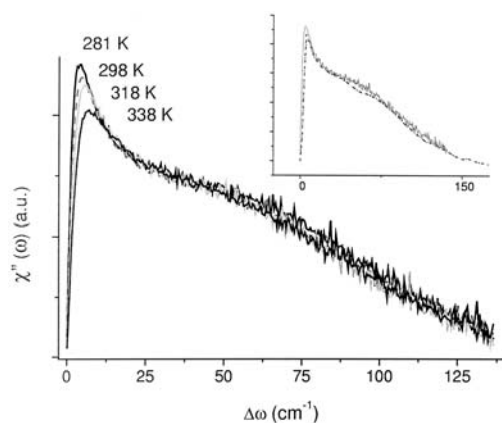


**Fig. 2.** Spectral susceptibility of  $\text{CH}_3\text{CN}$ , at different temperatures, obtained correcting the corresponding DRS spectra for the quantity  $(\nu - \nu_0)^4 [n(\nu) + 1]$ , where  $n(\nu)$  is the Bose factor. In the inset the reduced DRS spectrum at 298 K (dotted line) is compared to the FT of the OHD-OKE signal measured at the same temperature (dashed line). The two spectra perfectly overlap except for the very low frequency region.

Quartz cells of 1 cm optical path length and selected for minimum depolarization of light were utilized. These were inserted in a special copper holder kept at a temperature controlled within  $\pm 0.1$  K by flowing ethylene glycol from a thermostat.

The data were treated using the expression reported in many papers (see for example Ref. [9]). The OHD-OKE

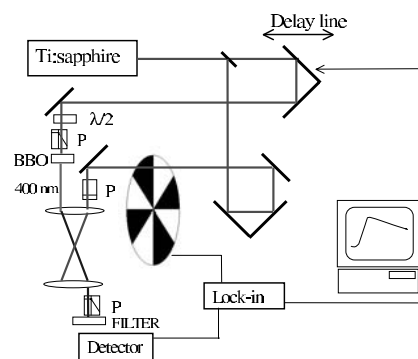


**Fig. 3.** Experimental apparatus for time resolved OHD-OKE.

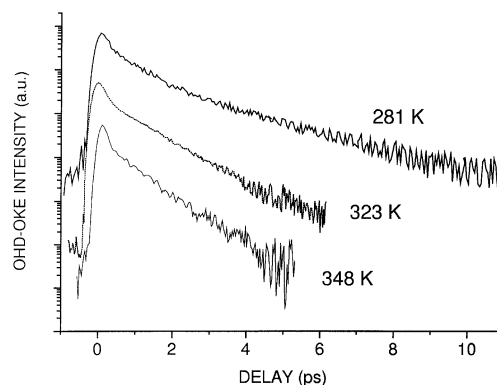


**Fig. 4.** The semi log plot of the OHD-OKE decay curves at different temperatures. The slow component is clearly fitted by a single exponential.

signal is given as

$$S(\tau) = \int_{-\infty}^{\infty} dt G(\tau - t) R(t) \quad (2)$$

where  $G(t)$  is the second order cross-correlation function as defined by equation (9) in the Appendix. In equation (2),  $R(t)$  is the molecular response proportional to the third order non-linear susceptibility.  $R(t)$  contains two contributions

$$R(t) = R_{\text{el}}(t) + R_{\text{nuc}}(t) \quad (3)$$

the first term on r.h.s. of equation (3) is the electronic contribution and, being instantaneous for the time resolution of our experiment, it is replaced by a  $\delta(t)$  function. The second term is the nuclear contribution to the signal. This is responsible for the delayed OKE signal and contains the relevant pieces of information about the dynamics of the liquid. In the present case the function providing the best fit of the experimental data is the sum of a non-exponential part plus a bi-exponential.

As a matter of fact, the choice of this form for  $R_{\text{nuc}}(t)$  is quite arbitrary. Apart from the long tail of the decay which is certainly exponential (see Fig. 4), the short time component, once that the long one is subtracted, can be fitted by an exponential function plus a damped oscillation (see Fig. 5). Such separation is not always possible.

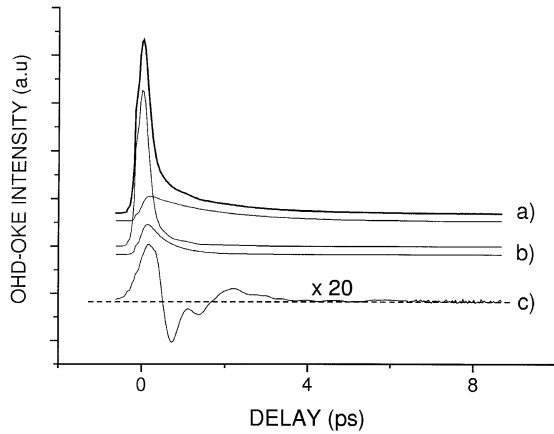


**Fig. 5.** The analysis of the OHD-OKE signal (experiment at 298 K). (a) The complete signal (upper trace) and the diffusive contribution only (lower trace). (b) The second contribution obtained by subtracting the diffusive part from the overall signal. Its simple exponential representation is reported below. (c) The remaining oscillatory part after subtraction of the short exponential component and of the electronic contribution.

Very often the damping constant of the oscillation is comparable to the decay constant of the pseudo-exponential part.

A more proper approach is that first proposed by McMorro [9], *i.e.* the analysis of the residual signal made in the frequency domain. Both these methods (time analysis and frequency analysis) are examined next.

Following a first rough estimate of the time constant of the long part of the decay, the slow component is exactly determined by fitting the OHD-OKE signal with the convolution function

$$S(t) = G(t) \otimes R_{\text{nuc}}^{\text{slow}}(t) \quad (4)$$

where

$$R_{\text{nuc}}^{\text{slow}}(t) = A \exp(-t/\tau) [1 - \exp(-t/\tau_R)]. \quad (5)$$

The time constants  $\tau$  and  $\tau_R$  are respectively the falling and rising edge of the response.  $\tau_R$  has been estimated to be below 100 fs (the average value is 90 fs) from two different and independent procedures. The first one, suggested in reference [22], is to adjust  $\tau_R$  in order to get a smooth decay of the imaginary part of the FT of the response function at high frequencies ( $\sim 200 \text{ cm}^{-1}$ ) as shown in Figure 7. The second is to take  $\tau_R$  equal to  $1/2\pi c \langle \Delta\omega \rangle$  where  $\langle \Delta\omega \rangle$  is the first moment of the spectral density obtained by taking the imaginary part of the FT of the total OHD-OKE signal [21] (one example is shown in the inset of Fig. 2). Both methods have a large relative uncertainty ( $\pm 30\%$ ) but the averaged values are almost the same.

$\tau$  and  $A$  are determined by fitting the tail of the decay with equation (4); after that,  $S(t)$  is subtracted by the OHD-OKE signal. The result of the subtraction is shown in the semi log plot of Figure 6.

The part resulting from the subtraction can be analyzed following two distinct methods. The first is to subtract a second exponential of the same form of equation (5)

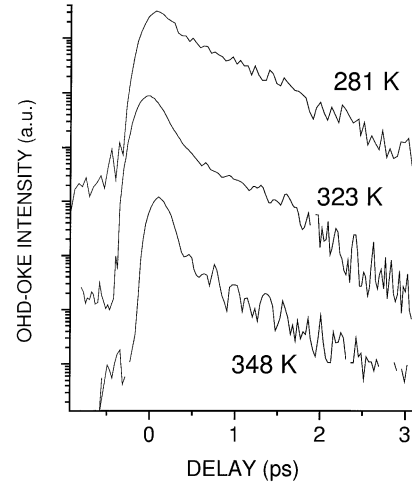


**Fig. 6.** The fast component of the OHD-OKE signal after the subtraction of the diffusive contribution. We observe that the weight relative to that of the electronic response decreases at increasing temperatures.

and convoluted with the instrumental function according to equation (4). This procedure allows to get a second decay time constant of the order of 500 fs, consistent with the values reported in reference [24]. The oscillating part resulting from the subtraction of the second exponential, which is visible in a restricted range of temperatures and after averaging several measurements, (see bottom of Fig. 5) can be approximately reproduced by the convolution of the instrumental function with a damped sine function with frequency of about  $25 \text{ cm}^{-1}$  and decay constant of 0.8 ps. Although affected by a large uncertainty, the damping constant is of the same order of magnitude of that of the decay of the shorter exponential.

The second method is that of taking the FT of the experimental data after the subtraction of the long exponential function. As already discussed in other papers, the uncertainty of the zero delay time position introduces some errors in the intensity ratios between the various spectral components [6,9]. We take the estimate of the zero delay obtained from equation (9) without any further adjustment. Tests on the sensitivity of the data to the change of the zero delay position show that in the low frequency range ( $< 200 \text{ cm}^{-1}$ ) the process does not introduce relevant errors. The spectra obtained through the above described technique show a broad feature almost unaffected by temperature with a maximum around  $50 \text{ cm}^{-1}$  (see Fig. 7) and a lower frequency peak which decreases in intensity with increasing temperature corresponding to the fast exponential decay of Figure 6.

### 3 Results and discussion

In Table 1 are collected the various dynamical parameters obtained by following the procedures described in the

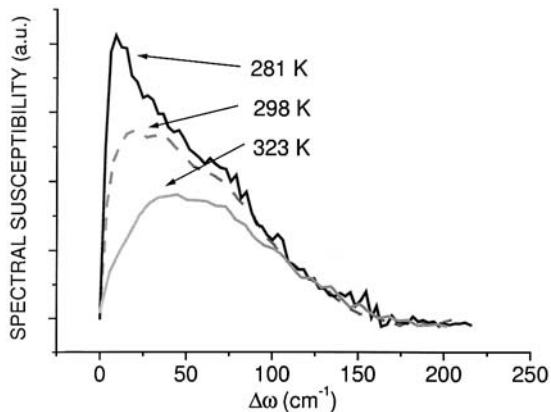


**Fig. 7.** The low frequency of the imaginary part of the FT of the short time OHD-OKE signal of Figure 6. The pronounced peak at 10  $\text{cm}^{-1}$  observed at 281 K decreases in intensity with increasing temperature as a consequence of the shortening and reduction of the weight of the fast component observed in the time domain.

**Table 1.** Characteristic times for the slow ( $\tau_{\text{or}}^{(2)}$ ) and fast ( $\tau_{\text{f}}$ ) decay components at different temperatures<sup>a</sup>.

T/K	CH <sub>3</sub> CN		CD <sub>3</sub> CN		
	OKE		Rayleigh	OKE <sup>b</sup>	Rayleigh <sup>c</sup>
	$\tau_{\text{f}}$ /ps	$\tau_{\text{or}}^{(2)}$ /ps	$\tau_{\text{or}}^{(2)}$ /ps	$\tau_{\text{or}}^{(2)}$ /ps	$\tau_{\text{or}}^{(2)}$ /ps
281	0.55(0.05)	2.0(0.1)	1.8(0.1)	2.1(0.2)	1.9(0.1)
293			1.5(0.1)		
298	0.50(0.05)	1.6(0.1)	1.5(0.1)	1.7(0.2)	1.5(0.1)
318		1.3(0.2) <sup>b</sup>	1.2(0.1)	1.3(0.2)	1.3(0.1)
323	0.40(0.05)	1.1(0.1)			
338	0.35(0.05)	1.0(0.1)	1.0(0.1)	1.0(0.2)	1.1(0.1)
348	0.3(0.1)	0.85(0.1)			

<sup>a</sup> Errors are reported in brackets, <sup>b</sup> homodyne detection, <sup>c</sup> from reference [27].

previous paragraph. The discussion is divided into two parts: one concerning the long ( $>1$  ps) exponential decay and the other concerning the dynamics below 1 ps.

### 3.1 The diffusive dynamics (long-time decay)

The extended analogy revealed in the long-time range of correlation functions deduced from depolarized Rayleigh scattering and in the time-resolved OHD-OKE decays, as reported in Table 1, suggests us to discuss and interpret this part of the orientational decay contextually and without distinction.

The DRS correlation functions and the OHD-OKE signal decays observed in molecular liquids are the manifestation of the fluctuations of the imaginary susceptibility. They reflect, at a molecular level, the relaxations of the molecular polarizability anisotropy caused by the different collective dynamical processes taking place in the liquid. Specifically, the long part of these polarizability

anisotropy time decays is described by the ensemble average  $\langle \beta^A(0); \beta^B(t) \rangle$  originated from the fluctuations of the molecular orientation  $G_m^{A,B}(t)$ :

$$\langle \beta^A(0); \beta^B(t) \rangle = \sum_{m=-2}^2 |\beta_m(MF)|^2 G_m^{A,B}(t). \quad (6)$$

The coefficients in equation (6) represent the spherical components of the static polarizability anisotropy (a second order tensor) and  $G_m^{A,B}(t)$  are functions describing the nature of the molecular dynamics. To the DRS profiles (as well as to the Raman anisotropic profiles of totalsymmetric bands) of symmetric top molecules only the  $m = 0$  term contribute [43]. It is associated with the reorientation of the molecular unique axis around the degenerate axes (tumbling motion). The presence of the indices  $A$  and  $B$  in equation (6) (which label distinct molecules in the liquid), point out the pair-particle character of the orientational correlation function  $G_m^{A,B}(t)$  extracted from these experiments. Separating the single molecule from the pair contribution the following expression is obtained:

$$\langle \beta^A(0); \beta^B(t) \rangle = \langle \beta^A(0); \beta^A(t) \rangle + \sum_{A \neq B} \langle \beta^A(0); \beta^B(t) \rangle. \quad (7)$$

In the limit of vanishing intermolecular correlation occurring when molecules are either intrinsically or extrinsically non interacting, only the first term in the r.h.s. of equation (7) survives; the consequence is that the long-time decay observed in these conditions directly gives the orientational autocorrelation (single particle) function.

It has been demonstrated that the separation of the correlation function  $\langle \beta^A(0); \beta^B(t) \rangle$  into two contributions does not imply two exponential functions [44, 45]. For symmetric top molecule, a single exponential is obtained in both the pure liquid and diluted solutions the only difference being that the decay time measured in the pure liquids is longer than in isoviscous diluted solutions. The ratio between the time measured in the pure liquid and that of a very diluted solution provides an estimate of the static Gierke factor [46]  $g^{(2)}$  according to  $\tau_p^{(2)} = g^{(2)} \tau_s^{(2)}$ . The lower value for the orientational relaxation time obtained in the present work by DRS experiments of CH<sub>3</sub>CN highly diluted in an iso-viscous mixture at 298 K ( $\tau_s^{(2)} = 1.2$  ps) respect to that obtained in neat acetonitrile at approximately the same temperature ( $\tau_p^{(2)} = 1.5$  ps) strongly suggests that molecules are locally organized ( $g^{(2)} > 1$ ). Incidentally we notice that the value obtained for the single particle orientational relaxation time closely compares to that obtained for the same dynamical parameter in a molecular dynamics calculation at the same temperature [47].

In the Debye theory it is assumed that the rotational diffusion is the result of a random walk process of succeeding infinitesimally short rotational steps. The extension of the theory to molecular systems where the latter condition does not fully applies was proposed, for linear molecules, by Gordon [48] with the  $J$  and  $M$  extended

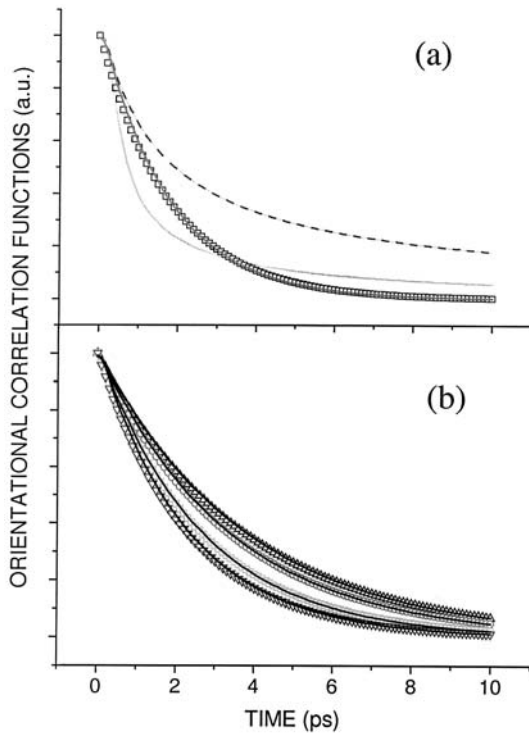


**Fig. 8.** (a) Comparison between the experimental (open squares) and the theoretical orientational correlation functions at 281 K. The  $J$ -model closely reproduces the experimental results for  $\tau_j^* = 0.1$  whereas the  $M$ -model fails to do it for the same parameter as well as  $\tau_j^* = 0.3$ . (b) Comparison between the experimental (symbols) and theoretical ( $J$ -model) orientational correlation functions at different temperatures.

models for describing the nature of the orientational dynamics in liquids in an extended range of regimes from the diffusive to the inertial limits. These models, successively elaborated by McClung [49] to include spherical and symmetric top molecules, are examples of a stochastic modelling of the orientational motion and of a collision interrupted random walk of the angular momentum. The picture of molecular reorientation offered by these models is that of molecules freely orientating during an elementary step interrupted by a random collisional event. The latter is instantaneous and causes a randomization either of the orientation ( $M$ -model) or of both the orientation and the magnitude ( $J$ -model) of angular momentum. Our results show that the more relevant difference between the two models is the different decay rate that is smaller for the  $M$ -model (Fig. 8a) as a consequence of the different averaging procedures over angular momentum. In the  $J$ -diffusion the average over  $J$  is performed at each collision while in the  $M$  diffusion after the last collision. This is the reason why the memory of  $J$  persists longer in the  $M$  diffusion model.

The duration of the diffusive steps are random and are assumed to follow a Poissonian distribution with characteristic time,  $\tau_j$  which is also the average time between collisions. Succeeding collisions are independent and no memory is retained in the sequence of collisional events. On the basis of the fundamental approach formulated by

Gordon, McClung derived the analytical form of the orientational correlation functions for symmetric top molecules that parametrically depends on a quantity  $\tau_j^*$  that is a measure of the prevalent regime in which any given system of orienting molecule in a liquid is found at any definite temperature. Since it represents the relative magnitude of the collisional time (measured by  $\tau_j$ ) respect to the molecular rotational period  $\tau_\omega$ , the inequalities  $\tau_j^* \gg 1$  and  $\tau_j^* \ll 1$  indicate the occurrence of the inertial and the diffusive regimes, respectively. Both models predict that the orientational correlation functions decay faster as  $\tau_j^*$  increases (see Figs. 8a and 8b) indicating a progressive achieving of the inertial regime ultimately represented by the free rotor decay of the orientational correlation. As the collisional time  $\tau_j$  gets longer respect to the molecular rotational period  $\tau_\omega$  progressively the molecular dynamics gets closer to the inertial regime. The opposite holds when the collisional time gets shorter than the rotational period: the diffusional regime comes progressively closer. It seems out of doubt that the  $M$ -model does not reproduce our orientational correlation functions, independently on the value of  $\tau_j^*$  (see Fig. 8a) while the  $J$ -model does it rather closely for all temperatures. The best value we have obtained for the parameter  $\tau_j^*$  at each temperatures fulfils the condition  $\tau_j^* \ll 1$  indicating that our molecular system experiences a diffusive dynamics in the explored thermodynamic conditions. Our results indicate that the  $\tau_j^*$  values increase with temperature, that the diffusive character of the orientational dynamics is more enhanced as the temperature decreases and that the collisional time  $\tau_j$  increases with temperature faster than the molecular rotational period  $\tau_\omega$ . Since this latter changes with  $T^{-1/2}$  and our results indicate that  $\tau_j^*$  changes approximately linearly with  $T$ ,  $\tau_j$  should change with  $T^{1/2}$ . To try to interpret at least qualitatively this conclusion we have considered the Enskog collision frequency [50]

$$\tau_E^{-1} = \left( \frac{kT}{\pi M} \right)^{1/2} 4\pi\rho\sigma^2 g(\sigma). \quad (8)$$

The model assumes that succeeding collisions are uncorrelated. The Enskog time  $\tau_E$  has an explicit temperature dependence ( $T^{-1/2}$ ) which cannot interpret our results but it implies an implicit temperature dependence through  $\rho$ . Our experiments are performed at variable temperature and in non-isochoric conditions. The change of particle density with temperature should be considered since it partly counteracts the explicit  $T^{-1/2}$  dependence of  $\tau_E$  and could offer a more adequate interpretation of the temperature dependence of our collisional time results.

### 3.2 The short time dynamics

The discussion concerning the short dynamics (also referred as the intermediate dynamics [24]) deserves some preliminary observations, only partly reported in the previous section. To get a more comprehensive picture it is helpful to collect them together and summarize according to the following four points.

(1) Once the long component of the decay has been subtracted, the signal shows unambiguously another decay that, within the experimental error, is described by an exponential decay law (see semi-log plot of Fig. 6). This part of the decay is particularly evident in the OHD-OKE signals over almost two decades of the intensity scale and is observable also in the first picosecond of the time correlation functions obtained from DRS spectra at least at low temperatures (see insets of Fig. 1).

(2) The intensity of the fast component, defined as the product of the pre-exponential factor times the decay constant, and normalized to the intensity of the electronic (instantaneous) component, strongly decreases with increasing temperatures becoming almost unobservable at 75 °C. The intensity of the electronic component can be considered an internal reference standard. Unfortunately it is difficult to make an absolute measurement of it. However it is a reasonable assumption that it scales as the density of the liquid. This means that its contribution decreases only of about 5% going from 8 to 65 °C. The intensity of the fast component decreases of more than 50% in the same interval, therefore leading to the conclusion that it is very sensitive to temperature. Its nature is related to density but also and probably to the most part to some other property connected to the structure of the liquid. On the contrary, the intensity of the long component is definitely less sensitive to temperature.

(3) In some data sets and in a very narrow temperature range (10–50 °C) a weak, damped oscillation is observed on top of the decay (see Fig. 5). The oscillation is clearly discernible at 25 °C and has been fitted with a damped sine function whose best parameters values are  $25 \pm 5 \text{ cm}^{-1}$  for the central frequency and  $700 \pm 200 \text{ fs}$  for the decay constant. Because of the weakness of the signal it is difficult to provide the dependence of the decay constant and of the central frequency with temperature.

(4) The analysis in the frequency domain of the signal shows a broad feature with a maximum around  $50 \text{ cm}^{-1}$  and a narrower band peaked around  $20 \text{ cm}^{-1}$  which is more evident once the diffusive contribution is subtracted. This latter component should correspond to the short exponential decay. Its intensity decreases rapidly with increasing temperature as expected. The position of the broad band is rather insensitive to the temperature changes (see Figs. 2 and 7).

In many simple liquids, fast signals superimposed to those due to the diffusive dynamics and occurring on time scales shorter than 1 ps are usually observed. It has been recently experimentally verified that at least in symmetric top molecular liquids the law describing the short relaxation dynamics is exponential [24]. The origin of such dynamical processes is undoubtedly connected to the intermolecular interactions.

The four points summarized at the beginning of this section are consistent with a model which takes into account two different contributions. The first one is due to inhomogeneous broadened oscillators coherently excited by the laser pulses. This contributes to part of the short decay and is the origin of the broad band centered at

$50 \text{ cm}^{-1}$ . The simplest picture of these oscillators is that of molecules liberating and vibrating in differently distributed environments (cages with different structure and dynamics). The second contribution must be due to a particular structure which can be easily identified among the numerous structures randomly distributed in the liquid. The strong pair correlation proved by other techniques [51–53] and also by the comparison between the dynamics of the pure liquid and that of the isoviscous solution show unambiguously the presence of dimers. By increasing the temperature the dimers become less stable and their contribution to the overall dynamics decreases.

## 4 Conclusions

In this paper we have presented a study of the dynamics of pure liquid acetonitrile in a wide temperature range. The complex relaxation pattern has been analyzed by dividing it into two parts. The long decay part is well reproduced by adopting the  $J$  extended diffusion model. From the analysis we find that the average collisional time increases with temperature as a consequence of the decreasing of the density of the liquid. However in the temperature range of the present experiment the condition  $\tau_j^* \ll 1$  is always verified indicating the diffusive nature of the process. The fast decay component has a complex origin. The simplest model capable of describing this dynamics is that of dephasing processes affecting the coherently excited liberating and oscillating molecules in the solvent cage. In the case of acetonitrile, the strong temperature dependence of the intensity of the short decay part of the signal and the necessity of introducing a  $g^{(2)}$  factor considerably greater than the unity to scale the pure liquid results to those of isoviscous solutions, suggest that part of the signal is due to a vibrating dimer. This interpretation agrees with the model describing the structure of the liquid characterized by the presence of strong pair correlations.

This work has been supported by the Italian Consiglio Nazionale delle Ricerche (CNR) under the contract n. 97.03227.CT03, the Istituto Nazionale per la Fisica della Materia (INFM) and by the European Community under the contract HPRI-CT1999-00111. Professor McClung is acknowledged for the kind offer of his  $J$  and  $M$  model calculation program. The authors wish to thank the LENS technical staff, M. De Pas and M. Giuntini of the electronic shop and of R. Ballerini and A. Hajeb of the machine shop for their essential contribution.

## Appendix: The dual color OHD-OKE experiment

In this appendix some details of the dual color OHD-OKE experiment will be provided. The instrumentation is based on a Ti:sapphire oscillator producing a train of 70 fs pulses at 800 nm with an average power of 1 W at a repetition rate of 82 MHz. A 80/20 beam splitter produces two beams: the pump and the probe. The pump

beam passes through a half wave plate, a calcite polarizer and is focussed by a 100 mm thin lens in the sample to generate the optical anisotropy. A pair of LaKL21 glass Brewster angle prisms are placed at the output of the laser, and their relative distance adjusted to achieve the shortest duration of the pump pulse on the sample (75 fs). The pulse duration is measured by second harmonic autocorrelation in a thin (100  $\mu\text{m}$ ) BBO crystal and results to be well reproduced by a Gaussian curve. The spectrum measured in the same position has also a Gaussian shape and a bandwidth 1.2 times the Fourier limit.

The probe impinges on the sample after passing a delay line (0.5  $\mu\text{m}$  resolution), a half-waveplate, a calcite polarizer at  $45^\circ$  respect to the polarizer of the pump and a thin (300  $\mu\text{m}$ ) frequency doubling BBO crystal. The signal is measured through a crossed polarizer in respect to the polarization direction of the frequency doubled pulse. A filter in front of the PMT detector remove the radiation at the fundamental (800 nm).

The dual color configuration has advantages and disadvantages. It certainly achieves a better contrast and therefore allows to extend the observation of the longer (weaker) dynamics. However, being the central wavelengths of the two pulses far apart and utilizing a thick sample one has to face the problem of group velocity mismatch (GVM) [54,55]. The OHD-OKE technique is very sensitive and allows to measure directly signal proportional to the response function of the system and therefore the data analysis results simpler [1–13, 16, 17, 19, 21, 22, 24, 25, 42, 47]. Generally the local oscillator on the detector is obtained by rotating the first polarizer on the probe beam (typically  $\pm 1$  degree). In the present case the small depolarization caused by the frequency doubling process provides always a leak through the analyzer. The relative phase of this local field cannot be controlled as in the case of the rotation of the preparing polarizer. To achieve the same control the polarization of the pump must be rotated: two measurements are performed in sequence with the pump once vertical and the other horizontal. Such situation results analogous to that generally described in literature: it is observed a change in the sign of the signal. The heterodyne signal is measured by a lock-in amplifier in phase with the modulation of the pump achieved by the insertion of a mechanical chopper (chopping frequency 3000 Hz).

The time resolution of the setup measured by THG cross-correlation in a thin BBO crystal placed in the sample region is 200 fs (FWHM) corresponding to a probe duration of 190 fs. We observe a fairly symmetric shape confirming the Gaussian nature of the laser pulses. The spectrum of the blue pulse is almost Gaussian in shape and the product duration-bandwidth is 2.2. This is due to the chirping of the blue pulse (the system is optimized for the duration of the pump). Any attempt to compensate for this chirping introduces experimental complications that are not worth to. This could be a limitation of the dual color experiment if the system is not stable. A second limitation is the effect of GVM which always occurs when two pulses far apart in terms of central frequency are utilized.

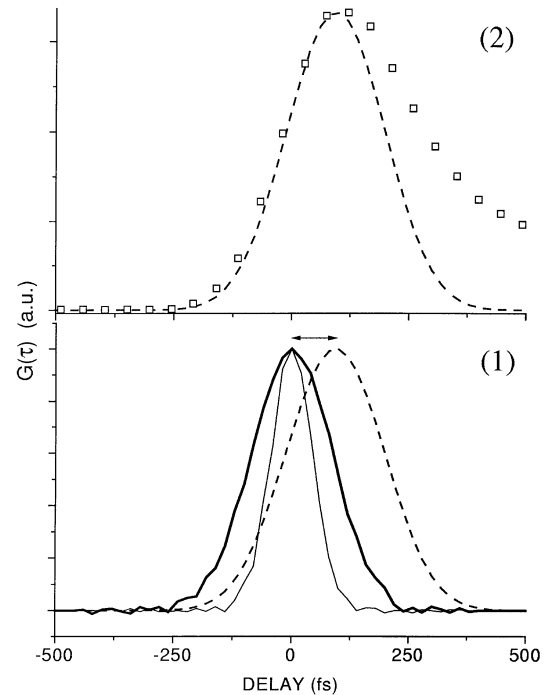


**Fig. 9.** The cross-correlation function between pump (800 nm) and probe (400 nm) pulses. (1) The autocorrelation of 800 nm pulses (thin line) is compared to the cross correlation function in a thin BBO crystal (thick line) and to the cross-correlation function calculated including GVM effects (dashed line). (2) The calculated cross-correlation function (dashed line) is compared to the experimental OHD-OKE signal (open squares): the rise parts of the two functions perfectly overlap.

The way to overpass this problem is to model the effect of GVM in order to better analyze the experimental data.

If we compare the rise of the THG signal and that of the OKE it is apparent that the latter is slower (see Fig. 9(1)). This is due to the fact that because of GVM the pump and the probe pulses travel at different speed in the medium. As a result the cross-correlation function broaden (see Fig. 9(2)). As discussed in reference [43] the effect of GVM can be easily calculated in the case of Gaussian pulses. The cross-correlation function  $G(t)$  is given by

$$G(\tau) = \frac{c}{a\Delta n} \left\{ \text{erf} \left[ a \left( \tau + \frac{\ell}{c} \Delta n \right) \right] - \text{erf}(a\tau) \right\} \quad (9)$$

where  $\Delta n$  is the difference between the indexes of refraction of the medium at, in the present case, 400 nm and 800 nm;  $\ell$  is the length of the interaction volume;  $a = 2\sqrt{\ln 2 / (\Delta\tau_{\text{pump}}^2 + \Delta\tau_{\text{probe}}^2)}$ ; ( $\Delta\tau$  is the duration of the pulses FWHM). The effect of GVM is compared in Figure 9(1) to the cross-correlation obtained in a thin BBO crystal.

Starting from a cross-correlation function of 200 fs, corresponding to a duration of the probe of 190 fs, a 2 mm length of the interacting volume (an estimate consistent with the optical parameters of the experiment) broaden the instrumental function up to 230 fs and shifts the zero

delay time of about 50 fs. This is the main effect and results important in the data analysis. When the system is stable, such broadening of the instrumental function can be perfectly compensated during the analysis process.

## References

1. W.T. Lotshaw, D. McMorrow, C. Kalpouzos, G.A. Kenney-Wallace, *Chem. Phys. Lett.* **136**, 323 (1987)
2. D. McMorrow, W.T. Lotshaw, G.A. Kenney-Wallace, *J. Quant. Electron.* **QE-24**, 443 (1988)
3. C. Kalpouzos, W.T. Lotshaw, D. McMorrow, G.A. Kenney-Wallace, *J. Phys. Chem.* **90**, 6893 (1989)
4. W.T. Lotshaw, D. McMorrow, *J. Chem. Phys.* **93**, 2160 (1990)
5. D. McMorrow, W.T. Lotshaw, *Chem. Phys. Lett.* **174**, 85 (1990)
6. D. McMorrow, W.T. Lotshaw, *J. Phys. Chem.* **95**, 10395 (1991)
7. D. McMorrow, W.T. Lotshaw, *Chem. Phys. Lett.* **178**, 69 (1991)
8. T. Hattori, A. Terasaki, T. Kobayashi, T. Wada, A. Yamada, H. Sasabe, *J. Chem. Phys.* **95**, 937 (1991)
9. D. McMorrow, *Opt. Commun.* **86**, 236 (1991)
10. M. Cho, S.J. Rosenthal, N.F. Scherer, L.D. Ziegler, G. Fleming, *J. Chem. Phys.* **96**, 5033 (1992)
11. D. McMorrow, W.T. Lotshaw, *Chem. Phys. Lett.* **201**, 369 (1993)
12. Y.J. Chang, E.W. Castner Jr, *J. Chem. Phys.* **99**, 113 (1993)
13. Y.J. Chang, E.W. Castner Jr, *J. Chem. Phys.* **99**, 7289 (1993)
14. M. Cho, M. Du, N.F. Scherer, G.R. Fleming, S. Mukamel, *J. Chem. Phys.* **99**, 2410 (1993)
15. R.S. Cataliotti, P. Foggi, M.G. Giorgini, L. Mariani, A. Morresi, G. Paliani, *J. Chem. Phys.* **98**, 4372 (1993)
16. Y.J. Chang, E.W. Castner Jr, *J. Phys. Chem.* **98**, 9712 (1994)
17. S. Palese, L. Schilling, R.J.D. Miller, R.P. Staver, W.T. Lotshaw, *J. Phys. Chem.* **89**, 6308 (1994)
18. B.M. Ladanyi, Y.Q. Liang, *J. Chem. Phys.* **103**, 6325 (1995)
19. W.T. Lotshaw, D. McMorrow, N. Thantu, J.S. Melinger, R. Kitchenham, *J. Raman Spectr.* **26**, 571 (1995)
20. M.G. Giorgini, P. Foggi, R.S. Cataliotti, A.R. Distefano, A. Morresi, L. Mariani, *J. Chem. Phys.* **102**, 8763 (1995)
21. E.L. Quitevis, M. Neelakandan, *J. Phys. Chem.* **100**, 10005 (1996)
22. R.A. Farrer, B.J. Loughnane, L.A. Deschenes, J.T. Fourkas, *J. Chem. Phys.* **106**, 6901 (1997)
23. J.C. Deak, L.K. Iwaki, D.D. Dlott, *J. Phys. Chem. A* **102**, 8193 (1998)
24. B.J. Loughnane, A. Scodinu, R.A. Farrer, J.T. Fourkas, U. Mohanty, *J. Chem. Phys.* **111**, 2686 (1999)
25. P. Bartolini, M. Ricci, R. Torre, R. Righini, I. Santa, *J. Chem. Phys.* **110**, 8662 (1999)
26. S.L. Whittenburg, C.H. Wang, *J. Chem. Phys.* **66**, 4255 (1977)
27. M.G. Giorgini, A. Morresi, L. Mariani, R.S. Cataliotti, *J. Raman Spectr.* **26**, 601 (1995)
28. P. Sassi, G. Paliani, R.S. Cataliotti, *J. Chem. Phys.* **108**, 10197 (1988)
29. P. Sassi, A. Morresi, G. Paliani, R.S. Cataliotti, *J. Raman Spectr.* **30**, 501 (1999)
30. E. Marri, A. Morresi, G. Paliani, R.S. Cataliotti, M.G. Giorgini, *Chem. Phys.* **243**, 323 (1999)
31. A. Morresi, P. Sassi, M. Ombelli, G. Paliani, R.S. Cataliotti, *Phys. Chem. Chem. Phys.* **2**, 2857 (2000)
32. R.S. Cataliotti, P. Sassi, A. Morresi, G. Paliani, *Chem. Phys.* **255**, 8 (2000)
33. P. Sassi, A. Morresi, G. Paliani, R.S. Cataliotti, *J. Phys.: Cond. Matt.* **12**, 3615 (2000)
34. A. Morresi, P. Sassi, M. Paolantoni, S. Santini, R.S. Cataliotti, *Chem. Phys.* **254**, 337 (2000)
35. S. Kinoshita, Y. Kai, M. Yamaguchi, Y. Yagi, *Phys. Rev. Lett.* **75**, 148 (1995)
36. R.G. Gordon, *J. Chem. Phys.* **42**, 3658 (1964)
37. R.G. Gordon, *J. Chem. Phys.* **43**, 1307 (1965)
38. R.G. Gordon, *Adv. Magn. Reson.* **3**, 1 (1968)
39. R.W. Hellwarth, *Prog. Quant. Electron.* **5**, 1 (1977)
40. D. Kivelson, P.A. Madden, *Ann. Rev. Phys. Chem.* **31**, 523 (1980)
41. O. Faurskov Nielsen, *Ann. Rep. Roy. Soc. Chem.* **90**, (1993)
42. P. Foggi, M. Bellini, D.P. Kien, I. Verduque, R. Righini, *J. Phys. Chem.* **101**, 7029 (1997)
43. F.J. Bartoli, T.A. Litovitz, *J. Chem. Phys.* **56**, 413 (1971)
44. T. Keyes, D. Kivelson, *J. Chem. Phys.* **56**, 1057 (1972)
45. G.R. Alms, D.R. Bauer, J.I. Brauman, R. Pecora, *J. Chem. Phys.* **59**, 5310 (1973)
46. T.D. Gierke, *J. Chem. Phys.* **65**, 3873 (1976)
47. H.J. Bohm, I.R. McDonald, P.A. Madden, *Mol. Phys.* **49**, 347 (1983)
48. R.G. Gordon, *J. Chem. Phys.* **44**, 1830 (1966)
49. T.E. Eagles, R.E.D. McClung, *Chem. Phys. Lett.* **22**, 414 (1973)
50. W.G. Rothschild, *Dynamics of Molecular Liquids* (Wiley, New York, 1984)
51. A. Kratochwill, J. Weider, H. Zimmermann, *Ber. Bunsenges. Phys. Chem.* **77**, 408 (1973)
52. H. Bertagnolli, M.D. Zeidler, *Mol. Phys.* **35**, 177 (1978)
53. T. Radnai, S. Itho, H. Otaki, *Bull. Chem. Soc. Jpn.* **61**, 3485 (1988)
54. F.V.R. Neuwahl, L. Bussotti, P. Foggi, in *Research Advances in Photochemistry and Photobiology* (Global Research Network, Trivandrum, Kerala, India, 2000), p. 77
55. J.C. Diels, W. Rudolf, *Ultrashort Laser Pulse Phenomena* (Academic Press, New York, 1996)